VOLUME 5, NUMBER 4, APRIL 2005

© Copyright 2005 by the American Chemical Society

NANO LETTERS

Correlation between Surface Photovoltage and Blend Morphology in Polyfluorene-Based Photodiodes

Marco Chiesa, Lukas Bürgi,† Ji-Seon Kim, Rafi Shikler, Richard H. Friend, and Henning Sirringhaus*

Cavendish Laboratory, Madingley Road, Cambridge CB3 0HE, United Kingdom

Received December 14, 2004

ABSTRACT

We present a microscopic study of photoinduced charge generation in polyfluorene-based photovoltaic structures. The sub-100 nm lateral resolution of scanning Kelvin probe microscopy allows characterizing the three-dimensional structure of thin films of blends of poly-(9,9′-dioctylfluorene-*co*-benzothiadiazole) (F8BT) and poly-(9,9′-dioctylfluorene-*co*-bis-N,N′-(4-butylphenyl)-bis-*N,N*′-phenyl-1,4-phenylenediamine) (PFB). From the strong correlation between surface photovoltage and blend morphology, we propose a simple model for the lateral and vertical film structure identifying in particular those regions with the most efficient conduction pathway for the photocurrent.

Organic material-based solar cells are an interesting alternative to traditional photovoltaic materials such as silicon because of their simplicity and low-cost of manufacture. Efficient charge photogeneration can occur by exciton dissociation at the heterojunction between dissimilar materials present in both bilayer and blend devices. High power conversion and external quantum efficiencies have been obtained[1] in devices using blends of hole- and electron-accepting conjugated polymers. The electronic properties of the individual materials as well as the morphology of demixed polymer blends are key factors for the device efficiency and performance.[2] In particular, transport pathways for both photogenerated excitons as well as charges are strongly affected by changes in the morphology.[3] Therefore, a better understanding of the correlation between blend morphology associated with transport pathways and the photovoltage measured on a macroscopic diode structure is needed in order to improve device performance.

In this work, noncontact scanning Kelvin probe microscopy (SKPM) has been used as a tool to measure the surface potential and the photoinduced surface photovoltage with a lateral resolution better than 100 nm and correlate this with the topography of the blend devices. The high lateral resolution of SKPM allows to measure directly spatial variations of the electrical properties of the devices and to gain insight in the operation mechanisms which cannot be obtained from macroscopic data of finished devices. SKPM has been previously used to study surface photovoltage[4] in inorganic semiconductors[5] and in organic self-assembled monolayers deposited on metal films.[6] It has also been found to be a very powerful potentiometric tool to investigate the

* Corresponding author. E-mail: hs220@phy.cam.ac.uk; Tel. +44 1223 337557; Fax +44 1223 353397.

† Present address: CSEM SA, Badenerstrasse 569, 8048 Zürich, Switzerland.

10.1021/nl047929s CCC: $30.25 © 2005 American Chemical Society
Published on Web 03/11/2005

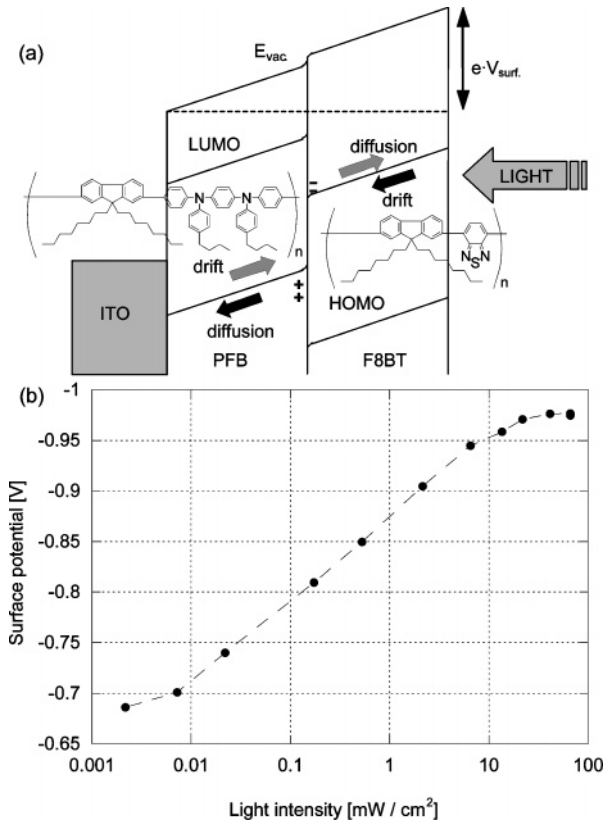

Figure 1. (a) Schematic energy level diagram for a bilayer structure under illumination at open circuit. The chemical structures of PFB and F8BT are also shown. (b) The intensity dependence of V_{surf} of the bilayer at room temperature with excitation at 473 nm as measured by SKPM.

device physics of organic transistors.[7−9] SKPM uses a noncontact atomic-force microscope tip with a conducting coating to measure the difference between the tip potential and the local surface potential with high spatial resolution of less than 100 nm. Our setup uses a frequency modulation technique in ultrahigh vacuum. Further details about the experiment are reported elsewhere.[7,10]

Polyfluorene-based conjugated polymers are interesting materials for photovoltaic applications because of their chemical stability, charge transport properties, and ease of controlling electronic structure through copolymerization.[11] The polyfluorene-based polymers used in this work are the high-mobility hole-transporting material poly-(9,9′-dioctylfluorene-*co*-bis-*N*,*N*′-(4-butylphenyl)-bis-*N*,*N*′-phenyl-1,4-phenylenediamine)[12] (PFB) and the electron-transporting polymer poly-(9,9′-dioctylfluorene-*co*-benzothiadiazole)[13] (F8BT). The chemical structures of these two polymers are shown in the inset of Figure 1(a). These materials have been used successfully to fabricate photovoltaic cells with maximum external quantum efficiencies of 22% (at 335 nm)[14] due to efficient dissociation of the exciton at the polymer−polymer heterojunctions[2,11] followed by charge transfer. Although a number of different device structures have been proposed, they belong mainly to two classes: structures with (quasi-) planar polymer−polymer heterojunctions, such as bilayers,[15,16] or with distributed heterojunctions, such as polymer blends.[17,18] The short-circuit current and the open-circuit voltage are among the key factors determining the power conversion efficiency of photovoltaic cells. Bilayers are a good model system due to their structural simplicity. The origin of the open-circuit voltage in solar cells based on bilayers of PFB and F8BT on indium−tin oxide (ITO) substrates has been investigated by Ramsdale et al.[16] and, in particular, a component logarithmically dependent on the illumination intensity has been observed. The distributed heterojunctions present in polymer blend devices result in a larger interfacial area between the two different polymer components than in bilayers, thus favoring charge separation and, therefore, higher short-circuit current. On the other hand, the open-circuit voltage in blend devices is lower than in bilayers, due to direct paths between cathode and anode within either phase acting as a shunt resistor in parallel with the active part of the device.[19] Therefore, to fabricate efficient devices, care needs to be taken to ensure bicontinuous pathways for electron and hole charge transport from the heterointerface to the respective contacts.

We first validated the use of SKPM by comparing the surface photovoltage as measured by SKPM with the open-circuit voltage of a photovoltaic cell[16] using simple bilayer structures. PFB was spun directly onto the ITO substrate, while F8BT was spun onto a mica substrate, floated off into deionized water and laminated onto the PFB layer.[16] No cathode electrode was put on top in order to have the F8BT surface directly accessible by the SKPM probe. Figure 1a shows schematically the model of a bilayer structure under illumination under open circuit conditions. Photogenerated excitons diffuse and charge separation occurs at the polymer−polymer heterojunction. This results in a charge concentration gradient within each layer. Under open circuit conditions the diffusion current of charges away from the interface must be balanced by a drift current caused by the internal electric field built up in the device so that the total current is zero, thus resulting in a net contact potential difference/surface photovoltage between the ITO anode and the F8BT surface. The surface potential of the bilayer as a function of the intensity of the illumination impinging on the device is shown in Figure 1b. The illumination source is a laser diode with a maximum intensity of 140 mW/cm^2, a spot size of 870 μm fwhm, and a wavelength of 473 nm, close to the absorption peak of F8BT.[18] The relationship between the surface potential and the illumination intensity is logarithmic, in good agreement with previous results,[16] establishing SKPM as a suitable technique to study charge separation processes in polymer photocells.

Polymer blend devices were prepared by spin-casting from a 1:1 solution (15 g/L concentration) of F8BT and PFB in *p*-xylene on an oxygen-plasma cleaned ITO-coated glass substrate. The molecular weights of the polymers used are M_n = 112 kg/mol for F8BT and 60 kg/mol for PFB, respectively. Figure 2a shows the topography of the device. Two phases with relatively large feature sizes (up to a few microns) can be clearly distinguished, one PFB-rich (the lower (darker) and closed-topology phase) and the other F8BT-rich (the higher phase constituting the continuous matrix).[20] The height contrast between the two phases is

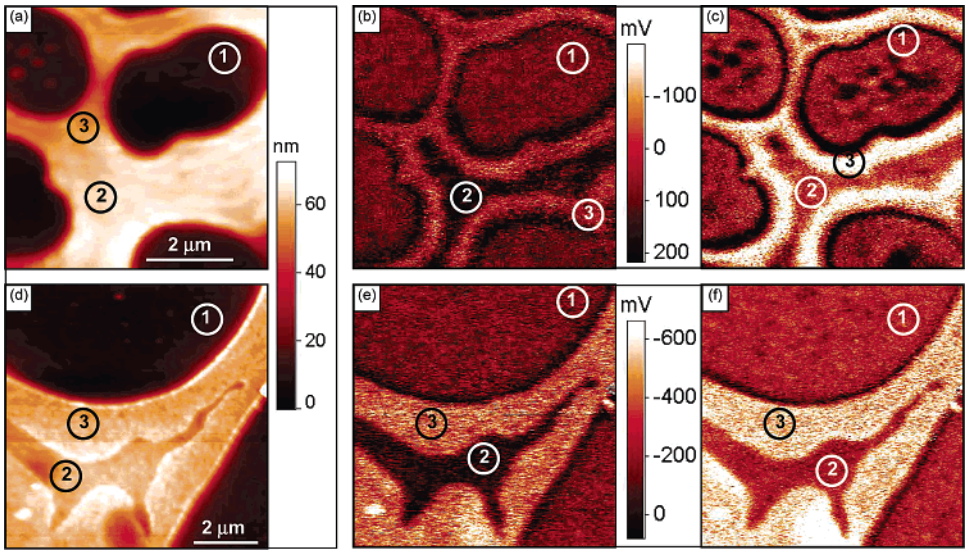

Figure 2. SKPM images of thin films of F8BT/PFB blends on top of the ITO anode prepared by spin coating (a−c) and in saturated solvent atmosphere (d−f): topography (a,d) and surface potential measured, respectively, in the dark (b,e) and illuminated with a 7 mW/cm^2 473 nm laser (c,f). Darker levels correspond to more positive and lighter levels to more negative surface potentials. Regions marked 1, 2, and 3 are, respectively PFB-rich, "bulk" and "interfacial" F8BT-rich phases. The difference in the absolute values is due to variations in the tip work function between measurements.

about 50 nm. Each phase has been found to substantially penetrate through the film to the underlying substrate.[17] However, the phases are not pure but a finer scale of phase separation of the order of tens of nm is contained in each of them.[11] This much finer scale of phase separation is responsible for most of the charge generation since it matches the short diffusion length of the exciton (a few nm).[21] Figures 2b and 2c show the corresponding surface potential measured, respectively, in the dark and under illumination at 473 nm. Ideally, in dark conditions, no charges are expected to be present in the blend, and therefore the energy bands should not be bent; the surface potential should be constant across the device, and equal to the work function difference between the SKPM tip and the ITO bottom electrode. However, Figure 2b shows that, at the boundary between the PFB-rich (1) macrophase and the bulk region in the F8BT-rich macrophase (2), there is an interface region (3) on the F8BT side of the boundary, which has a more negative potential than the bulk phases. This implies that part of the photogenerated charge does not recombine and remains trapped in the device under dark conditions. Trapped charge is generated each time the device is illuminated; our setup, however, does not allow us to measure a completely "fresh" device because of stray ambient light. When the device is illuminated, free charges are photogenerated at the polymer/polymer heterojunctions after dissociation of the excitons. Charge separation occurs not only at the interface between the macrophases, but also within each macrophase due to the fine-scale phase separation. For example, in the PFB-rich phase holes diffuse and eventually reach the ITO anode while electrons diffuse to the surface in the F8BT regions embedded in the PFB-rich phase. Resolving potential differences due to this fine (probably of the order of 10 nm) phase separation is beyond the resolution limit of our SKPM setup. However, under illumination we do observe a more negative surface potential in *all* regions as compared to the values measured in the dark. At a wavelength of 473 nm where F8BT, but not PFB, is strongly absorbing, the surface potential is more negative in the F8BT than in the PFB macrophase, it is the highest in the interface region (3) between the two macrophases. The higher-potential (dark in the figure) rims around the PFB-rich phases visible in the potential images are "artifacts" due to the steep topographic contrast. Figures 2d, 2e, and 2f show, respectively, the topography and the surface potential in the dark and under illumination at 473 nm of a device prepared under saturated solvent atmosphere, in which phase separation is allowed to proceed to longer length scales approaching thermodynamic equilibrium. Figure 2d shows clearly that the bulk-F8BT phase (2) and the interface F8BT phase (3) exhibit different surface topography, with a height difference of about 5 nm. The clear correlation between the topography and the potential distribution indicates that the devices are constituted by three regions, namely the PFB-rich (1), the "bulk" (2), and the "interfacial" (3) F8BT-rich phases.

The relation between the surface potential in the different regions and the intensity of illumination is shown in Figure 3a. The dependence is logarithmic in all the regions, with slopes of about −0.05 V/decade in the PFB-rich and in the "interfacial" F8BT-rich phases and of −0.08 V/decade in the "bulk" F8BT-rich phase, which are consistent with the bilayer data.[16] The potential in the PFB-rich region saturates at relatively low intensity (3 mW/cm^2), when the minority F8BT phases become saturated with electrons. We have also measured the time dependence of the potential in the dark in the different regions and have observed relatively long time scales for the decay of the surface potential (Figure 3b). The potential in the different regions is plotted as a function of the time elapsed since light switch-off. The potential in the "bulk" phases (both PFB- and F8BT-rich) decays with long time constants toward the equilibrium condition, while the potential in the "interfacial" F8BT-rich region returns comparatively quickly to its equilibrium value

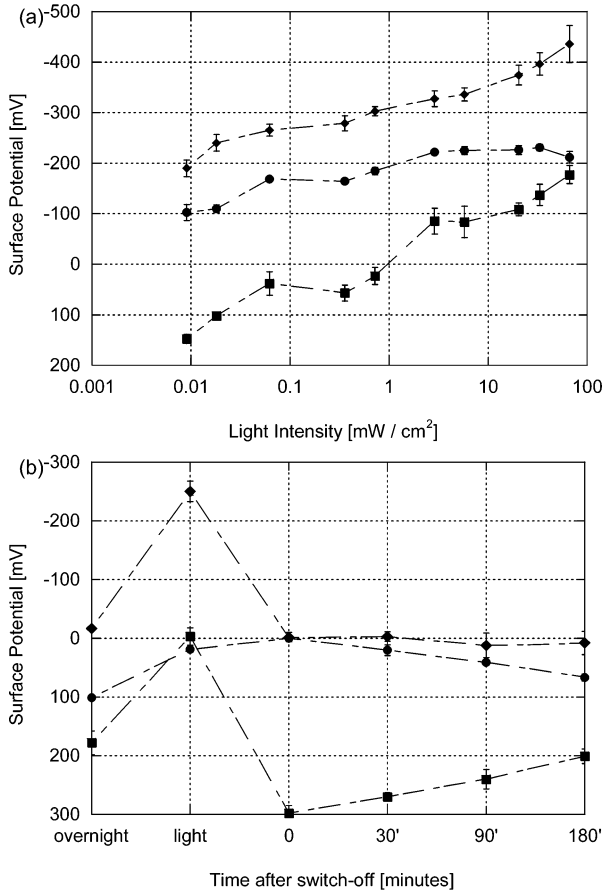

Figure 3. (a) The intensity dependence of V_{surf} in the blend at room temperature with excitation at 473 nm in the PFB-rich (circles), bulk (squares), and interfacial (diamonds) F8BT-rich phases. (b) The time dependence of V_{surf} in the dark in the PFB-rich (circles), bulk (squares), and interfacial (diamonds) F8BT-rich phases. The points marked "light" have been measured at 7 mW/cm^2. The differences between the absolute values in (a) and (b) arise since data come from different samples and from variations in the tip work function. However, the trends are similar for different samples.

in the dark. The long decay times in the other bulk regions are likely due to the slow release of the charge present in trap states populated by the photogenerated carriers. The difference in the detrapping dynamics strongly supports the idea of a morphological difference between the "interfacial" and the "bulk" F8BT-rich regions.

To understand the obtained results, not only the lateral but also the vertical phase separation of the polymer blend device must be taken into account. Detailed X-ray photoelectron spectroscopy (XPS)[22] studies performed on blends of F8BT and poly-(9,9′-dioctylfluorene-*co*-(1,4-phenylene-((4-*sec*-butylphenyl)imino)-1,4-phenylene)) (TFB), a material with thin-film properties similar to PFB, has shown the presence of both a TFB-rich wetting layer at the polymer−ITO interface and a TFB-rich capping layer at the polymer−air interface. While the TFB wetting layer is continuous and uniform, the capping layer does not cover the whole film but only forms isolated pockets over the primary F8BT-rich phases. This complex morphology is believed to be driven by different surface energy and solubility between the two dissimilar polymers.[22] A similar surface enrichment by the

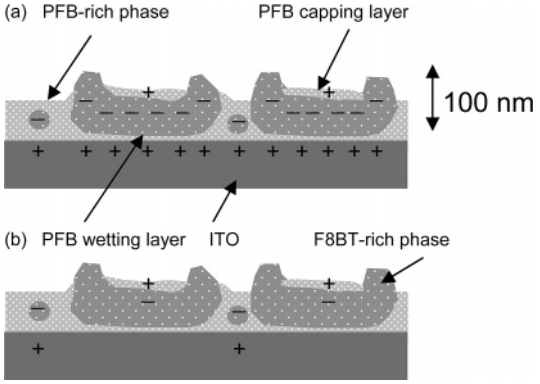

Figure 4. Proposed model of the blend thin film structure. (a) Schematic charge distribution under illumination. (b) Distribution of the slow-recombining trapped charge after light switch-off.

low surface energy component has been also observed in blends of F8BT and poly-(9,9′-dioctylfluorene) (PFO).[23] Our results suggest that a similar self-organized vertical structure, schematically shown in Figure 4, is also formed in F8BT/PFB blends, with PFB as the lower surface energy component.[24] In particular, the PFB capping layer only covers the "bulk" F8BT-rich region (region (2) of Figure 2).

A model correlating the morphology and the charge generation and recombination in F8BT/PFB blend thin films for illumination at 473 nm has been developed. The charge distributions upon illumination and after switching off the light are schematically shown, respectively, in Figures 4a and 4b. In this simple, 1D-model the three phases, PFB-rich, "bulk", and "interfacial" F8BT-rich, are considered separately and being independent one of each other. Upon illumination, the photogenerated holes in the PFB-rich phase and wetting layer have a direct path to the ITO electrode and can be successfully extracted. On the other hand, holes in the PFB-rich capping layer and electrons in the F8BT-rich phase and in the F8BT pockets present in the PFB-rich phase are accumulated. As a consequence, the ITO anode gets positively charged and the polymer phases get negatively charged. On the other hand, a small positive charge is present in the PFB capping layer covering the "bulk" F8BT-rich region. The screening effect of these positive charges makes the potential in the "bulk" F8BT-rich region less negative than in the "interfacial" F8BT-rich region.

When the light is switched off, the negative charges present in the F8BT-rich phase recombine quickly with holes injected from the anode via the PFB wetting layer, while electrons in the PFB-rich bulk phase and holes in the PFB-rich capping layer are trapped in states, probably of polaronic nature. Only in the F8BT-rich interface region do photogenerated electrons have an efficient transport pathway in the dark to recombine with holes in the PFB wetting layer, which explains the fast decay of the surface potential in this region. In the other regions, the release of trapped charges manifests itself in a much slower relaxation of the dark potential. The sign of the slope of the decay of the potential is directly related to the sign of the slowly recombining surface charges. In particular, in the "bulk" F8BT-rich phase, the slow recombination of the holes left in the PFB capping layer makes the potential evolve toward less positive values; vice versa,

in the PFB-rich phase, the recombination of the electrons causes the potential to decay toward less negative values.

In conclusion, our SKPM investigations confirm previous results which have shown evidence for both lateral as well as vertical phase separation resulting in a complex morphology with a discontinuous capping layer being formed on the surface. We have shown directly that the presence of this capping layer reduces the efficiency of the photovoltaic device by blocking the transport of photogenerated electrons to the surface. The highest surface photovoltage in the blend film is being generated in the regions where a simple bilayer structure is present, suggesting that an efficient conduction path for photogenerated electrons is crucial for achieving a high device efficiency. We have also found evidence for the existence of trapped charges present in the dark for many hours after illumination in those regions in which no efficient path for recombination at the anode is present. This provides further confirmation for the structural model of the complex blend morphology. To which extent these trapped charges limit the efficiency and stability of a photovoltaic diode with a top cathode will be investigated in future work.

Acknowledgment. The authors thank the Engineering and Physical Sciences Research Council and the Epson Cambridge Laboratory for financial support and H. J. Snaith for valuable discussions. J.S.K. thanks the EPSRC via an Advanced Research Fellowship. M.C. thanks the EU−RTN Laminate for funding.

References

(1) Shaheen, S. E.; Brabec, C. J.; Sariciftci, N. S.; Padinger, F.; Fromherz, T.; Hummelen, J. C. *Appl. Phys. Lett.* **2001**, *78*, 841−843.
(2) Halls, J. J. M.; Arias, A. C.; MacKenzie, J. D.; Wu, W.; Inbasekaran, M.; Woo, E. P.; Friend, R. H. *Adv. Mater.* **2000**, *12*, 498−502.
(3) Snaith, H. J.; Friend, R. H. *Thin Solid Films* **2004**, *451*−*452*, 567−571.
(4) Kronik, L.; Shapira, Y. *Surf. Sci. Rep.* **1999**, *37*, 1−206.
(5) Weaver, J. M. R.; Wickramasinghe, H. K. *J. Vac. Sci. Technol. B* **1991**, *9*, 1562−1565.
(6) Cao, J.; Sun, J.-Z.; Hong, J.; Yang, X.-G.; Chen, H.-Z.; Wang, M. *Appl. Phys. Lett.* **2003**, *83*, 1896−1898.
(7) Bürgi, L.; Sirringhaus, H.; Friend, R. H. *Appl. Phys. Lett.* **2002**, *80*, 2913−2915.
(8) Bürgi, L.; Friend, R. H.; Sirringhaus, H. *Appl. Phys. Lett.* **2003**, *82*, 1482−1484.
(9) Bürgi, L.; Richards, T. J.; Friend, R. H.; Sirringhaus, H. *J. Appl. Phys.* **2003**, *94*, 6129−6137.
(10) Nonnenmacher, M.; O'Boyle, M. P.; Wickramasinghe, H. K. *Appl. Phys. Lett.* **1991**, *58*, 2921−2923.
(11) Arias, A. C.; MacKenzie, J. D.; Stevenson, R.; Halls, J. J. M.; Inbasekaran, M.; Woo, E. P.; Richards, D.; Friend, R. H. *Macromolecules* **2001**, *34*, 6005−6013.
(12) Redecker, M.; Bradley, D. D. C.; Inbasekaran, M.; Wu, W. W.; Woo, E. P. *Adv. Mater.* **1999**, *11*, 241−246.
(13) He, Y.; Gong, S.; Hattori, R.; Kanicki, J. *Appl. Phys. Lett.* **1999**, *74*, 2265−2267.
(14) Arias, A. C.; Corcoran, N.; Banach, M.; Friend, R. H.; MacKenzie, J. D.; Huck, W. T. S. *Appl. Phys. Lett.* **2002**, *80*, 1695−1697.
(15) Sariciftci, N. S.; Braun, D.; Zhang, C.; Srdanov, V. I.; Heeger, A. J.; Stucky, G.; Wudl, F. *Appl. Phys. Lett.* **1993**, *62*, 585−587.
(16) Ramsdale, C. M.; Barker, J. A.; Arias, A. C.; MacKenzie, J. D.; Friend, R. H.; Greenham, N. C. *J. Appl. Phys.* **2002**, *92*, 4266−4270.
(17) Halls, J. J. M.; Walsh, C. A.; Greenham, N. C.; Marseglia, E. A.; Friend, R. H.; Moratti, S. C.; Holmes, A. B. *Nature* **1995**, *376*, 498−500.
(18) Snaith, H. J.; Arias, A. C.; Morteani, A. C.; Silva, C.; Friend, R. H. *Nano Lett.* **2002**, *2*, 1353−1357.
(19) Snaith, H. J.; Greenham, N. C.; Friend, R. H. *Adv. Mater.* **2004**, *16*, 1640−1645.
(20) Stevenson, R.; Arias, A. C.; Ramsdale, C.; MacKenzie, J. D.; Richards, D. *Appl. Phys. Lett.* **2001**, *79*, 2178−2180.
(21) Stevens, M. A.; Silva, C.; Russell, D. M.; Friend, R. H. *Phys. Rev. B* **2001**, *63*, 165213.
(22) Kim, J.-S.; Ho, P. K. H.; Murphy, C. E.; Friend, R. H. *Macromolecules* **2004**, *37*, 2861−2871.
(23) Chappell, J.; Lidzey, D. G.; Jukes, P. C.; Higgins, A. M.; Thompson, R. L.; O'Connor, S.; Grizzi, I.; Fletcher, R.; O'Brien, J.; Geoghegan, M.; Jones, R. A. L. *Nat. Mater.* **2003**, *2*, 616−621.
(24) Ramsdale, C. M.; Bache, I. C.; MacKenzie, J. D.; Thomas, D. S.; Arias, A. C.; Donald, A. M.; Friend, R. H.; Greenham, N. C. *Physica E* **2002**, *14*, 268−271.

NL047929S